Proc. Annual Meeting of the Austrian Society for Biomedical Engineering 2021
DOI: 10.3217/978-3-85125-826-4-01

MODEL-BASED DEVELOPMENT OF A CLOSED-LOOP HEART RATE CONTROL STRATEGY USING VAGUS NERVE STIMULATION

M. Haberbusch[1,2], B. Kronsteiner[1,2], A. Kiss[2], F. Moscato[1,2,3]

[1]Center for Medical Physics and Biomedical Engineering, Medical University of Vienna, Vienna, Austria
[2]Ludwig Boltzmann Institute for Cardiovascular Research, Vienna, Austria
[3]Austrian Cluster for Tissue Regeneration, Vienna, Austria

max.haberbusch@meduniwien.ac.at

Abstract— *A previously developed numerical model of the cardiovascular system was applied to develop and compare two strategies for closed-loop heart rate control using vagus nerve stimulation in complete vagal-cardiac denervation. The strategies were also tested in a first pilot experiment in an anesthetized rabbit that underwent bilateral vagotomy. In-silico and ex-vivo experiment results were compared to evaluate the performance of the control strategies concerning* accuracy and settling time*. For both control strategies, the simulations led to performance indicators within the pre-defined requirements (10 bpm mean-squared error, 10% percentual overshoot, and 15 s settling time). In the in-vivo experiment, however, only one of the two control strategies could meet the requirements.*

Keywords— *numerical model, cardiac denervation, cardiovascular system, vagus nerve stimulation, closed-loop heart rate control.*

Introduction

In the past years, numerical models have gained increasing importance in the field of biomedical engineering. These models do not only help to better understand underlying mechanisms of human physiology and pathophysiology but also to develop novel treatment strategies and medical devices. Many successful examples of such computer simulations can be found in cardiovascular- [1],[2] and neural engineering [3],[4]. Although for long time models of both fields were typically separated representations of isolated physiological systems, in recent years, the interplay of the autonomic nervous- and the cardiovascular system is increasingly becoming a focus of interest, leading to integrated neuro-cardiovascular system models. Such models can not only improve our understanding of the autonomic control of the cardiovascular system in healthy individuals but also elucidate the hemodynamic and neurological changes associated with pathological conditions such as cardiac denervation resulting from e.g., diabetes mellitus or cardiac transplantation. From an engineering perspective, these models are of preeminent importance for the development of novel neuro-modulation-based treatment strategies for the conditions associated with cardiac denervation. Therefore, we applied a previously developed integrated numerical model [5],[6] that allows us to simulate the provoked acute cardiovascular effects of vagus nerve stimulation (VNS). This model was tuned and validated to reproduce the acute chronotropic response to VNS in rabbits that underwent bilateral vagotomy. The model was employed to develop two control strategies for closed-loop heart rate control using VNS in case of complete vagal-cardiac denervation. The model-based control strategies were evaluated in one pilot animal experiment.

Methods

Model overview: The developed model integrates a lumped-parameter representation of the cardiovascular system with its autonomic and intrinsic cardiac control and a model of cervical vagus nerve stimulation. In brief, the hemodynamic system model consists of modified Windkessel models representing the arterial and venous compartments of the systemic and pulmonary circulation. The atria and ventricles are realized as time-varying elastance models. The autonomic cardiac control is governed by the arterial baroreflex and the pulmonary stretch reflex. The intrinsic cardiac control is realized through a single-cell Hodgkin-Huxley-type sinoatrial node cell modeld. To simulate the acute cardiac effects of VNS, a multi-axon multi-compartment Chiu-Ritchie-Rogart-Stagg-Sweeney model [8] of an efferent vagal-cardiac nerve fiber population was implemented. Extracellular stimulation was realized by introducing an activation function as described by Rattay [9]. That model was coupled to a multi-compartment model of the ACh kinetics within the vagal-cardiac neuroeffector junctions [10]. The so-obtained ACh concentrations were then used to modulate the heart rate through changes in sinoatrial ion-channel gating behavior. The influence on atrioventricular conduction and ventricular contractility was implemented as a time-delay and first-order low-pass filter dynamics. An overview of the model can be found in Figure1.

Control Strategies: Two closed-loop heart rate control strategies were implemented using the previously described in-silico model: (a) unsynchronized VNS, and (b) cardiac-synchronized VNS. Briefly, in both control strategies, charge-balanced cathodic-anodic biphasic current pulses are delivered to the vagus

Published by Verlag der TU Graz
Graz University of Technology

DOI: 10.3217/978-3-85125-826-4-01

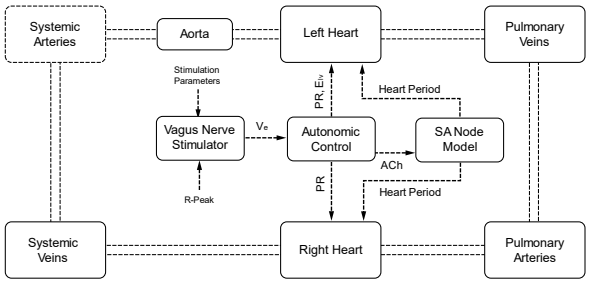

Figure 1: Overview of the integrated model (PR, atrioventricular conduction time; E_{lv}, left ventricular elastance, ACh, acetylcholine, V_e, extracellular potential).

nerve. In the unsynchronized control strategy, the stimulation is applied continuously without respect to the cardiac cycle. The shape of the pulses is determined by three main parameters: current amplitude (C), pulse width (PW), and frequency (F). In the synchronized strategy, a defined number of pulses (NP) is delivered with a specific delay (D) to the onset of left ventricular isovolumic contraction identified from the R-peaks in the electrocardiogram (ECG). A summary of the stimulation parameter values used is given in Table 1.

Table 1: Stimulation parameter values used in unsynchronized (U) and cardiac-synchronized (S) stimulation strategies.

Type	C (mA)	PW (µs)	F (Hz)	NP	D (ms)
U	0 – 2	200	30	-	-
S	0 – 2	200	30	8	0

The closed-loop control was implemented using a proportional-integral (PI) controller that minimizes the error between the measured instantaneous heart rate and a given reference heart rate. A previously performed sensitivity analysis highlighted the preeminent influence of the current amplitude on the provoked chronotropic responses [6], thus it was chosen as the control variable. The controller tries to minimize the perceived error by applying a correcting proportional and integrating term that are added to the current amplitude. The final form of the PI controller is given by Equation 1, where $P_c(t)$, is the controller output (current amplitude respectively), K_p is the proportional gain, K_i is the integral term, $e(t) = HR_{ref} - HR(t)$ is the error between the reference and the measured instantaneous heart rate.

$$P_c(t) = K_p e(t) + K_i \int e(t)dt \qquad (1)$$

Controller Gain Identification: The goal was to optimize the controller gains (K_p, K_i) concerning the accuracy and speed of convergence of the controller. Therefore, similar to the work of Ugalde et al. [11], the gains were optimized with regards to three performance indicators: (a) mean squared error (MSE) calculated from the last 10 s of the stimulation period, (b) percentual overshoot (%OS) corresponding to the overshoot amplitude expressed as a percentage of the final reference heart rate, and (c) the settling time (T_s) defined as the time that is required for the heart rate to go from baseline to 90% of the final value. Therefore, the cost function of the form:

$$F = \frac{1}{3}\left(\frac{MSE}{\widehat{MSE}} + \frac{\%OS}{\widehat{\%OS}} + \frac{T_s}{\widehat{T_s}}\right) \qquad (2)$$

was minimized using Bayesian optimization with 100 evaluations of the cost function. The cost function is defined as the arithmetic mean of the three performance indicators. The performance indicators were normalized to the respective requirements for the individual markers ($\widehat{MSE}$, $\widehat{\%OS}$, $\widehat{T_s}$). The predefined requirements were a maximum rise time of 15 s, a maximum relative overshoot of 10%, and a mean squared error below 10 bpm. For each optimization iteration, a step-response simulation was performed consisting of an initial phase of 100 seconds in which the controller is turned off to establish a baseline, followed by a phase of 100 seconds in which the controller is turned on, trying to reduce the heart rate by 35 bpm from baseline.

The optimization was carried out to meet the demands regarding the accuracy and settling time of the control strategy.

Hardware-in-the-loop implementation: Both control strategies were implemented using hardware-in-the-loop tools. The loop comprises an instrumentational amplifier (Warner DP-304A) to acquire the electrocardiogram (ECG) of the animal, a real-time prototyping system (DSPACE MicroLabBox) on which a binary of the control strategy is executed, a linear isolated stimulator (Biopac STMISOLA), and a bipolar cuff electrode used to deliver the stimuli to the animal's vagus nerve. A schematic overview of the hardware-in-the-loop chain is presented in Figure 2.

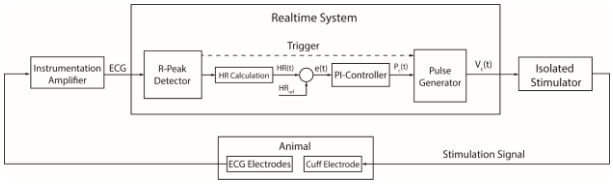

Figure 2: Schematic overview of the hardware-in-the-loop implementation of the control strategy.

Animal Preparation: One adult New Zealand white rabbit was used for initial evaluation of the control strategy under the approval of the Institutional Animal Care and Use Committee of the city of Vienna (BMBWF 2020-0.016.858 – GZ 2020-0.016.858).
The animal was premedicated with 0.1-0.2ml/kg ketamine (100mg/ml Ketasol®) and 0.2-0.3ml/kg dexme-

DOI: 10.3217/978-3-85125-826-4-01

detomidine (Dexdomitor®, 1mg/ml) injected intramuscularly, followed by intravenous induction of the same mixture via the auricular vein 15-20 minutes after premedication was given. The animal then was endotracheally intubated allowing anesthesia to be maintained with sevoflurane vaporized in a 40:60 mixture of oxygen and medical air.
For electrode implantation, the carotid sheath on the left and the right were opened and the trio consisting of the cervical vagus nerve (CVN), the internal jugular vein, and the common carotid artery were dissected, followed by gentle isolation of the CVN. Once both, the right and left CVN were exposed, a bipolar cuff-electrode (Microprobes NC-3.5-2-250P-5-6-sut-300-TP) with a diameter of 0.75 mm and contact spacing of 3 mm was wrapped around the right CVN with the anode positioned cephalad. After electrode implantation, both vagus nerves were dissected cephalad to the stimulation cuff electrode using surgical clippers.
The ECG was acquired using needle electrodes with anode and cathode placed on right and left upper limb respectively, and the reference electrode on the right hindlimb. Arterial pressure was monitored from the right femoral artery and mean arterial pressure was maintained in a range of 60 to 80 mmHg.

Control Test Procedure: To evaluate the performance of the control strategies using the controller gains identified from the in-silico model, a step-response test was performed. The protocol consisted of a single step from baseline, reducing the heart rate by 35 bpm. For the in-vivo experiment results, the performance indicators were calculated and compared to the predictions of the computer simulation.

Results

The gains of the PI controller were automatically tuned concerning accuracy and settling time using the in-silico model. After optimization, for both control strategies, all three performance indicators were well below the pre-defined requirements of 10 bpm, 10% and 15 s for MSE, %OS and T_s, respectively (Table 2).

Table 2: Optimal PI gains found by automatic optimization for unsynchronized (U) and cardiac-synchronized (S) stimulation strategies.

Type	K_p	K_i	MSE	%OS	T_s
U	0.001	0.005	2.7 bpm	3.5%	5.8 s
S	0.01	0.05	0.7 bpm	0.2%	3.8 s

Using the identified values for the controller gains, both control strategies were tested in one acute pilot experiment in an anesthetized rabbit that underwent bilateral vagotomy. Therefore, a step response protocol consisting of a single step was performed, decreasing the heart rate, starting from baseline by 35 bpm. The results of the step response protocol in the in-vivo experiments and that of the in-silico model are presented in Figure 3 and Figure 4 for the synchronized and the unsynchronized control strategy, respectively.

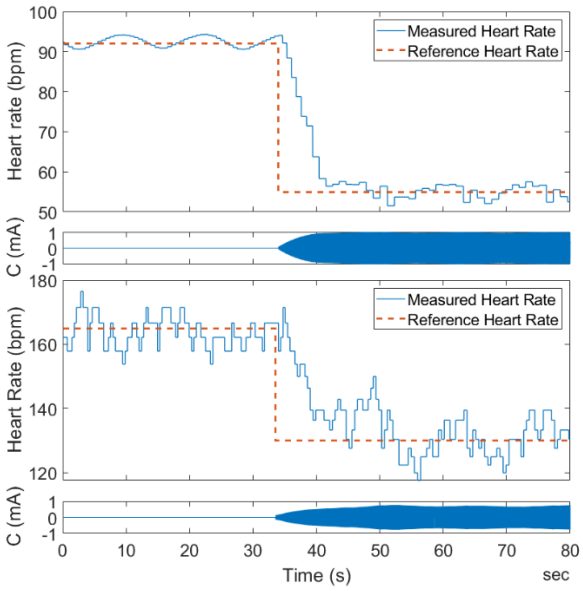

Figure 3: Step response using the unsynchronized control strategy in the in-silico model (top) and the in-vivo experiment (bottom).

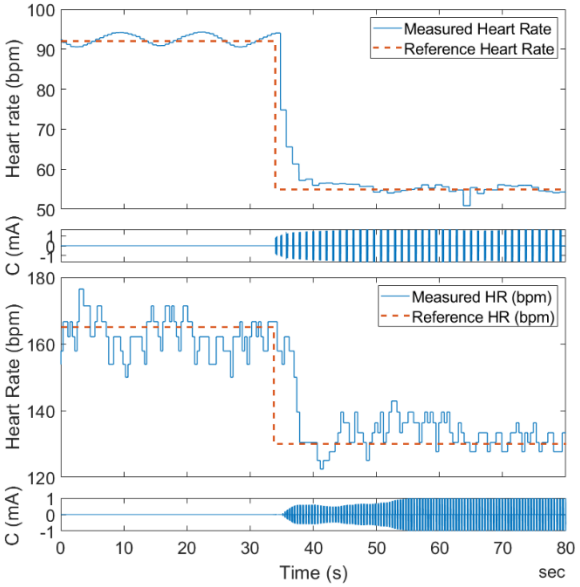

Figure 4: Step response using the cardiac-synchronized control strategy in the in-silico model (top) and the in-vivo experiment (bottom).

The three performance indicators (MSE, %OS, T_s) were also calculated for the in-vivo data. The results for the unsynchronized and the synchronized strategies are presented in Table 3. Both control strategies showed worse performance in the in-vivo experiments than predicted by the computer simulations. The synchronized control strategy however met all the pre-defined requirements while the unsynchronized type substantially exceeded the limits for the MSE.

Published by Verlag der TU Graz
Graz University of Technology

DOI: 10.3217/978-3-85125-826-4-01

Table 3: Performance indicators for in-vivo step response protocol using unsynchronized (U) and synchronized (S) stimulation strategies.

Type	MSE	%OS	T_s
U	22.9 bpm	2.3%	6.2 s
S	8.5 bpm	6.2%	4.3 s

Discussion

Numerical models have been proven to be viable tools to aid the development of medical devices and respective control strategies. In our work, we applied a previously developed numerical model that integrates the cardiovascular system and its autonomic control with a model of a vagal-cardiac nerve fiber population to develop two different control strategies for closed-loop heart rate control using VNS. These control strategies were then tested in a first pilot animal experiment.

The PI control was chosen over more sophisticated concepts as e.g., model predictive control due to its simplicity and straight-forward implementation. Although often a derivative term is added to the PI controller, it was omitted since previous studies suggest this leads to worse accuracy in closed-loop heart rate control [11].

The performance indicators calculated from the model predictions and the pilot in-vivo experiment for both control strategies lead to inconsistent results. Overall, the control strategies showed a substantially better performance in the computer simulations as compared to the pilot experiment. The discrepancies may be related to uncertain factors not considered in the numerical model such as anesthesia-related changes in dynamics of autonomic cardiovascular control. Thus, further investigations are needed to refine the computer model based on experimental results.

Although the performance of both control strategies was worse in the in-vivo experiment, the synchronized control strategy was markedly superior to the unsynchronized stimulation in terms of accuracy. Even though the performance was lower than predicted by the computer simulation, the synchronized control paradigm could meet all defined performance criteria suggesting it as a viable strategy for closed-loop heart rate control that should be pursued in future work.

Finally, we need to acknowledge limitations in our work. First, the baseline heart rate in the model was substantially different than that in the in-vivo experiments. This is because the intrinsic cardiac control of the model was realized as a human SA node model. We cannot exclude that using a sinoatrial node cell model of the rabbit would have improved the overall outcomes of the work. Moreover, the control strategy was only evaluated in a single animal. Therefore, we cannot draw any conclusions on the preservation of the control strategy performance for changed physiological conditions. Current work is focused on a refined tuning of the model for rabbit physiology and the evaluation of the control strategy in a virtual study population and later in a larger series of in-vivo experiments.

Overall, this work serves as a proof of concept of the capabilities of our model to aid the development and evaluation of novel VNS paradigms for the treatment of cardiovascular conditions associated with vagal-cardiac denervation.

Acknowledgments

This work was funded by the European Project H2020-EU.1.2.2. “A neuroprosthesis to restore the vagal-cardiac closed-loop connection after heart transplantation, NeuHeart” (Grant agreement ID: 824071).

References

[1] Y. Qian et al., “Computational hemodynamic analysis in congenital heart disease: simulation of the Norwood procedure,” Ann. Biomed. Eng., vol. 38, pp. 2302–2313, 2010.

[2] M. T. Politi et al., “The dicrotic notch analyzed by a numerical model,” Comput. Biol. Med., vol. 72, pp. 54–64, 2016.

[3] M. Sunshine et al., “Restoration of breathing after opioid overdose and spinal cord injury using temporal interference stimulation,” Commun. Biol., vol. 4, pp. 1–15, 2021.

[4] K. Aristovich et al., “Model-based geometrical optimisation and in vivo validation of a spatially selective multielectrode cuff array for vagus nerve neuromodulation,” J. Neurosci. Methods, vol. 352, pp. 109079, 2021.

[5] M. Haberbusch et al., ”Changes in Resting and Exercise Hemodynamics Early After Heart Transplantation: A Simulation Perspective,” Front. Physiol., vol. 11, pp. 1357, 2020.

[6] M. Haberbusch et al., “Towards Vagus Nerve Stimulation to Restore Heart Rate Control in Heart Transplant Patients: A Simulation Study,” in 18th Nordic Baltic Conference on Biomedical Engineering and Medical Physics, 2020.

[7] A. Fabbri et al., “Computational analysis of the human sinus node action potential: model development and effects of mutations,” J. Physiol., vol. 595, no. 7, pp. 2365–2396, 2017

[8] J. D. Sweeney et al., “Modeling of mammalian myelinated nerve for functional neuromuscular electrostimulation,” in IEEE 9-th ann. conf. Eng. Med. Biol., pp. 1577-1578, 1987.

[9] F. Rattay, Electrical Nerve Stimulation, Vienna, Austria: Springer-Verlag Wien, 1990.

[10] S. Dokos et al., "Vagal Control of Sinoatrial Rhythm: a Mathematical Model,” Journal of Theoretical Biology, vol. 182, pp. 21–44, 1996.

[11] H. M. R. Ugalde et al., “Model-Based Design and Experimental Validation of Control Modules for Neuromodulation Devices,” IEEE Trans. Biomed. Eng., vol. 63, no. 7, pp. 1551–1558, 2015

Published by Verlag der TU Graz
Graz University of Technology